Proceedings of 12th Cambridge Workshop on Cool Stars, Stellar Systems, & The Sun, 2003 University of Colorado.

XMM−Newton Spectroscopy of FK Comae

P. Gondoin, C. Erd, D. Lumb

Space Science Department, European Space Agency

Abstract.
FK Comae was observed twice at two weeks interval in January 2001 by the XMM−Newton space observatory. Analysis results suggest a scenario where the corona of FK Comae is dominated by magnetic structures similar in size to interconnecting loops between solar active regions but significantly hotter. The interaction of these structures themselves could explain the permanent flaring activity on large scales that is responsible for heating FK Comae plasma to high temperatures. During our observations, these flares were not randomly distributed on the star surface but were partly grouped within a large compact region of about 30 degree extent in longitude. We conjecture that this coronal region with a large density of flares could have been overlaying a large photospheric spot similar to those mapped using Doppler imaging techniques.

1. Introduction

FK Comae (HD 117155) is the prototype of a small group of single G giants defined by Bopp & Rucinski (1981) as the FK Comae-type stars. Its spectral peculiarities include a strong, broad and variable Hα emission (Walter & Basri 1982), a quasisinusoidal optical light curve, suggestive of starspots (Jetsu et al. 1993) and an X-ray luminosity (Welty & Ramsey 1994) exceptionaly high for a red giant. We report on analysis results of X−ray spectra of FK Comae registered during two observations performed in January 2001 by the XMM−Newton observatory. This work aims to improve our understanding of the magnetic activity on FK Comae by investigating the origin of FK Comae high X-ray luminosity and the structure of its X-ray corona.

2. Observations and Data Reduction

FK Comae was observed twice by the XMM−Newton space observatory (Jansen et al. 2001), respectively during revolution 199 on 2001 January 8 and during revolution 205 on 2001 January 21. Observations were conducted with the EPIC cameras (Strüder et al. 2001, Turner et al. 2001) operating in full frame mode ($E/\Delta E = 10$ to 60 in the 0.3 to 10 keV band). Spectra were recorded simultaneously with the RGS reflection grating spectrometers (den Herder et al. 2001) operating in the soft X-ray range ($E/\Delta E = 100$ to 50 in the 0.3 to 2.1 keV band).

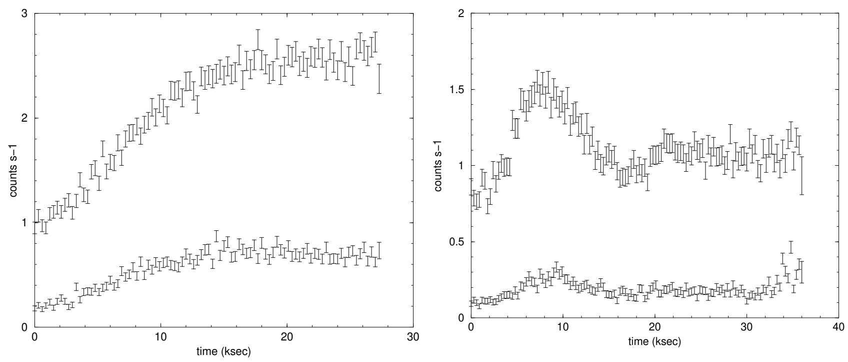

Figure 1. Light curve of FK Comae during revolution 199 (left) and 205 (right) obtained with the EPIC p−n camera. In each graph, the upper curve is the count rate within the 0.5 to 2 keV band and the lower curve is the count rate within the 2 to 10 keV band. The events are binned in 300 s time intervals.

Processing of the raw event dataset was performed using the XMM−Newton Science Analysis System (SAS version 5.0.1). The Pulse-Invariant (PI) spectra were rebinned such that each resultant MOS channel had at least 20 counts per bin and each p−n channel had at least 50 counts per bin. Spectral fitting was performed using the XSPEC package (v11) with EPIC response matrices provided by the PI institutes and with RGS response matrices generated by the SAS task "rgsrmfgen".

Table 1. X-ray luminosities (corrected for interstellar absorption) of FK Comae in the 0.3−2 keV and 2−10 keV energy bands during the different periods. The percentage contribution in luminosity of hot plasmas (kT >3 keV) is indicated between brackets.

Obs.	$L_{0.3-2keV}$ (10^{30} erg s^{-1})	$L_{2-10keV}$ (10^{30} erg s^{-1})	hr
Rev. 199 (rising cr)	28.1 (85%)	32.5 (99%)	0.07
Rev. 199 (high cr)	45.8 (92%)	55.1 (100%)	0.09
Rev. 205 (low cr)	18.3 (73%)	12.0 (98%)	-0.21
Rev. 205 (flare)	23.2 (73%)	17.8 (99%)	-0.13

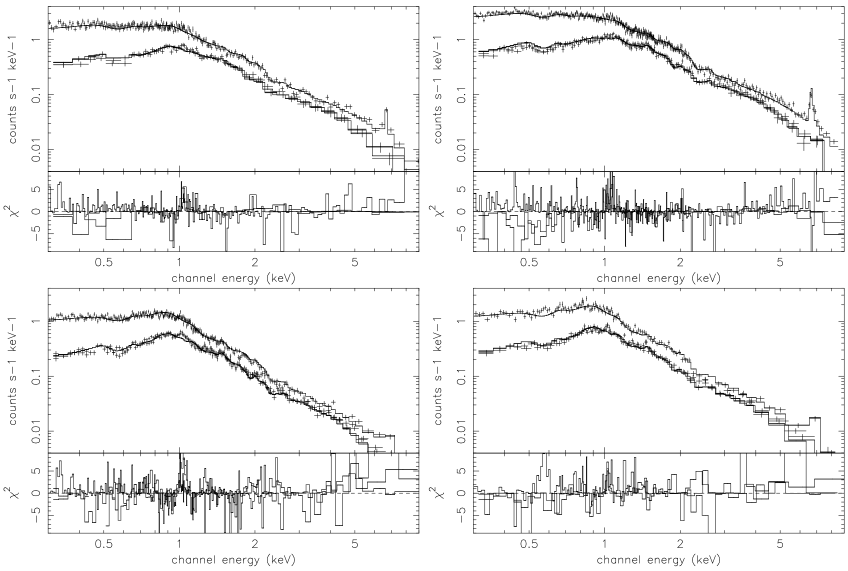

Figure 2. Top: best fit model to the EPIC spectra during the rising flux period (left) and during the high steady flux period (right) of revolution 199. Bottom: best fit model to the EPIC spectra during the low steady flux period (left) and during the short flare period (right) of revolution 205. The data and spectral fit are shown in the upper panel and the χ^2 contributions in the lower panel of each graph.

3. Integrated Flux and Temporal Behavior

Fig. 1 shows the light curves of FK Comae obtained during revolution 199 and 205 with the p−n camera. During revolution 199, the flux increased steadily during the first 15 ksec of the observation up to a high count rate which remained stable for the rest of the exposure. On the contrary, during revolution 205, the counts rates rapidly increased and decreased during the first 15 ksec of the observation and then remained stable at a relatively low level. Hence, we conducted the spectral analysis in each revolution for two flux levels. The spectral analysis of revolution 199 data was performed in two time intervals corresponding respectively to the slowly increasing flux period and to the steady high level flux period at the end of the observation. The spectral analysis of revolution 205 data was conducted in two time intervals corresponding respectively to the short transient flux increase at the beginning of the exposure and to the steady low flux level observed during the remaining part of the observation.

Spectral fitting during these four periods yields X-ray luminosities measurements in the 0.3−2 keV and 2−10 keV bands that are listed in Table 1, including hardness ratios. The hardness ratio hr of the X-ray emission ($hr = (L_{2-10keV} - L_{0.3-2keV})/(L_{2-10keV} + L_{0.3-2keV})$) was higher in revolution 199 than in revolution 205. In spite of a large increase in X-ray luminosity, hr did not change significantly during revolution 199. The relative increase of the X-ray flux was the same in the low and high energy band suggesting a ge-

Table 2. Best fit parameters to EPIC data using a 2 component MEKAL model and an hydrogen column density of 1.3 10^{-20} cm^{-3}

Obs.	Abundance	Low T	Component	High T	Component
		kT (keV)	EM ($10^{52}cm^{-3}$)	kT (keV)	EM ($10^{52}cm^{-3}$)
Rev. 199 (rising cr)	0.36±0.04	0.76±0.02	37±8	5.3±0.2	343±5
Rev. 199 (high cr)	0.52±0.03	0.74±0.02	23±3	4.8±0.1	585±5
Rev. 205 (low cr)	0.39±0.02	0.71±0.07	41±4	3.3±0.1	182±3
Rev. 205 (flare)	0.66±0.04	0.71±0.09	34±4	3.7±0.1	218±5

ometrical origin of the count rate variation. One possible explanation is the progressive emergence of bright X-ray material at the limb of the star. Since the flux increase duration was approximately 20 ksec compared with the 2.4 days stellar rotation period, the extent of this bright X-ray region would be about 30 degrees in longitude. According to this hypothesis, this region would have entered the visible hemisphere of FK Comae at the beginning of revolution 199 and would have been fully visible during the last 10 ksec of this revolution.

4. Spectral Analysis of EPIC Data

We separately fitted the four EPIC datasets (see Fig.2) with the MEKAL optically thin plasma emission model (Mewe et al. 1985). No single temperature plasma model that assumes either solar photospheric (Anders & Grevesse 1989) or non solar abundances can fit the data, as unacceptably large values of χ^2 were obtained. The MEKAL plasma models with two components at different temperatures prove adequate for all dataset (see Table 2). No improvement to the fit was obtained by adding a third temperature component.

The temperature of the cool plasma component is relatively constant (≈ 0.7 keV) for all datasets. Hot ($T > 3$ keV) plasma on FK Comae is the main source of X-ray emission both in the soft and in the hard X-ray bands. It contributes to more than 70 % of the soft X-ray luminosity in the 0.3−2 keV range and to more than 98 % of the luminosity above 2 keV (see Table 1). Table 2 shows that FK Comae's X-ray luminosity variations both in the soft (< 2 keV) and in the hard (>2 keV) range are almost entirely related to change in the emission measure of the hot ($T > 3$ keV) plasma whose temperature was higher during revolution 199 ($T \approx 5$ keV) when the X-ray luminosity was higher.

Assuming identical abundances in the two plasma components, the average element abundance in FK Comae corona is found to be lower than the solar photospheric value. However, the derived abundances are significantly higher during the high count rate periods of both revolution 199 and 205 data (Z=0.6±0.1) than during the respective low count rate periods (Z=0.37±0.05). This behavior is reminiscent of metallicity enhancements which have been reported during

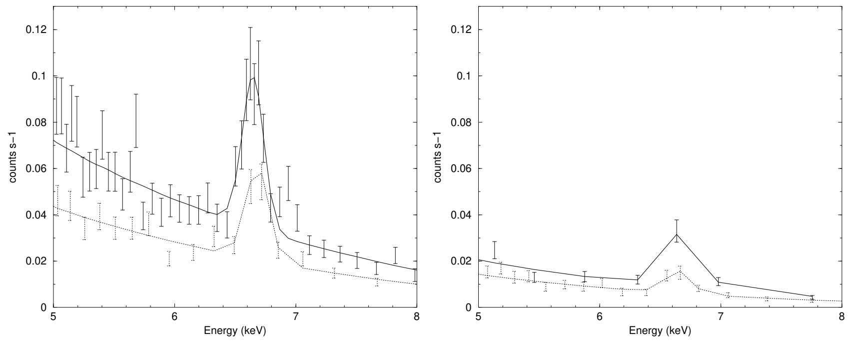

Figure 3. Profile of the Iron K line measured in revolution 199 (left) and in revolution 205 (right). The solid line represent the best fit in the 3 to 10 keV region by a phenomenological model consisting of a power law and a gaussian profile. The same scale have been used in both graphics to ease comparison.

stellar flares, e.g on Algol (Favata & Schmitt 1999) and on the RSCVn like binary II Peg (Mewe et al. 1997).

One major feature of FK Comae spectrum is the presence of a high energy tail and of an emission feature around 6.7 keV attributed to an iron K emission line (see Fig.3). The iron Kα fluorescent line energy is an increasing function of the ionization state. It rises slowly from 6.40 keV in Fe I to 6.45 keV in Fe XVII (neon-like) and then increases steeply with the escalating number of vacancies in the L-shell to 6.7 keV in Fe XXV and 6.9 keV in Fe XXVI (House 1969, Makishima 1986). The energy position of the FK Comae Fe K line at $6.67^{+0.04}_{-0.05}$ keV indicates that iron is in a high Fe XXV state of ionization. For a collisionally dominated optically thin coronal plasma, the Fe XXV ion concentration reaches a maximum value in the $2-7\ 10^7$ K temperature range (Raymond-Smith 1977), in agreement with the temperature of the hot plasma component derived by spectral fitting. The increase of the Fe K line peak intensity during the high count rate periods also indicates that the line is emitted by the hot plasma component. This confirms the thermal origin of the Fe K emission.

Among all of the different changes, eruptions and instabilities which are seen on the Sun, the ones which are labelled “flares” all have in common material heated to temperatures of 10^7K or greater (Golub & Pasachoff 1997). Thus, by analogy with the Sun, the existence of significant amounts of plasma at 10^7K in the corona of FK Comae and the detection of Fe XXV emission may be interpreted as basic flare indicators. The increase of the hot plasma emission measure and of its associated Fe XXV emission both during the short transient event of revolution 205 and during the steady flux increase in revolution 199 indicate that these two events are related to flaring activity. This is consistent with the view that the short transient event during revolution 205 is due to a single flare. On the other hand, the steady flux increase during revolution 199 could result from the gradual emergence of a large volume of hot plasma at the limb of the star corresponding to several flares occurring within the same region.

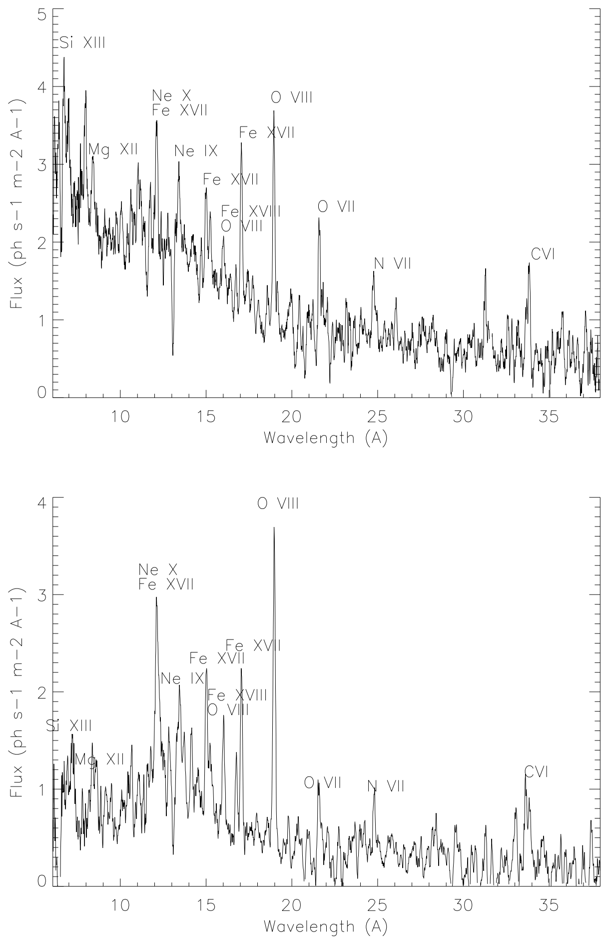

Figure 4. Averaged first order spectra of RGS 1 and 2 obtained during revolutions 199 (top) and 205 (bottom)

5. Spectral Analysis of RGS Data

Figure 4 shows the co-added spectra from RGS 1 and RGS 2 observations obtained during revolutions 199 and 205. Series of lines of highly ionized Fe and several lines of the H and He series are visible in the RGS spectra, most notably from C, N, O, and Ne. Their temperatures of maximum line formation range between 2 and 10 MK indicating that their are associated with the cool plasma component inferred from EPIC data. When comparing the spectra obtained during revolution 199 and 205, the most obvious difference is the higher continuum emission observed at short wavelengths during revolution 199. This continuum is mainly associated with the bremstrahlung emission from the high temperature ($T > 10^7$) plasma derived from EPIC data. The presence of a variable bremstrahlung component and of a stable line component in RGS spectra

Table 3. Best fit parameters to RGS spectra recorded in revolution 199 and 205 using a VMEKAL model with variable Fe, O and Ne abundance.

Parameter	Value
kT (keV)	0.76 ± 0.01
Fe	0.27 ± 0.01
O	0.33 ± 0.03
Ne	1.18 ± 0.14
Others	0.45
χ^2	1.16

support the use of a two temperature plasma model for the interpretation of the EPIC data.

Since the cool plasma component is responsible for the line emission spectrum of RGS and is relatively stable in temperature during revolution 199 and 205, we simultaneously fitted the low energy RGS spectra obtained in revolution 199 and 205 by an emission spectrum of hot diffuse gas based on the calculation of Mewe et al. (1985) with Fe L calculations by Liedahl (1995). The fit was performed in the spectral range from 10 $\AA$ to 20 $\AA$, where the efficiency of the RGS spectrometers is the highest. An initial abundance of 0.45 was used, as established by the MEKAL model. The temperature and abundances of the Fe, O and Ne elements which give prominent lines in the considered spectral range were then allowed to vary. The fitting results are given in Table 3. They corroborate the EPIC data analysis and indicate that the emission measure distribution of plasma in FK Comae exhibits a peak around 0.7 keV.

The average abundance derived from the RGS spectra is consistent with the EPIC data. However, the Ne abundance is significantly higher than the average value and the Fe and O abundances are slightly lower. Hence, the Ne/O ratio found for FK Comae is unusually high compared with the solar photospheric value. This Ne enhancement is reminiscent of a similar anomaly observed in a subset of solar flares (Schmelz 1993; Murphy et al. 1991).

Electron densities can be measured using density sensitive spectral lines originating from metastable levels, such as the forbidden (f) $2^3\mathrm{S}-1^1\mathrm{S}$ line in helium-like ions (Pradhan 1982; Mewe et al. 1985). The RGS wavelength band contains the He-like triplet from O VII, Ne IX, Mg XI and Si XIII. However, the Si and Mg triplets are not sufficiently resolved and the Ne IX triplet is too heavily blended with iron and nickel lines for unambiguous density analysis. Only the O VII lines are clean, resolved and potentially suited to diagnose plasmas in the density range $\mathrm{n}_e \approx 10^8$-$10^{11}$ cm^{-3} and temperature range $T \approx$ 1$-$9 MK. However, the temperature of the cool plasma component ($T \approx 0.75$ keV i.e 8.7 MK) is significantly larger than the temperature (T = 2 MK) of maximum abundance of the O VII ions, hence the low line intensities of the O VII triplet. This effect combined with the absence of RGS 2 data in this spectral range prevents an accurate measurement of the intercombination to forbidden line ratio. A rough estimate of the i/f ratio is 1.5 for revolution 199, which implies (Pradhan 1982) a density $n_e \approx 6\ 10^{10}$ cm^{-3} for a temperature of 0.75

keV. Unfortunately, the uncertainty on the i/f ratio only allows to ascertain a lower limit $n_e > 2\ 10^9$ cm^{-3} of the electron density during revolution 199. No estimate could be performed on the revolution 205 data due to the even lower flux.

6. Discussion

We argue that the XMM−Newton observations performed during revolution 205 recorded an X-ray flare on FK Comae. We interpreted the steady flux increase during revolution 199 as the gradual emergence of several flares at the limb of the star occurring within a localized region. Assuming that the emission measure increase of the hot component during revolution 205 is due to a single flare, the visible hemisphere of FK Comae could have been covered by more than 10 simultaneous giant flares at the end of revolution 199. The X-ray emission could also arise from more flare events of smaller size. The good fit to FK Comae spectra obtained with a two components models suggest a corona configuration with little contribution from quiet regions similar to the Sun. On the contrary the 0.7 keV temperature of the "cool" component is reminiscent of solar type active regions while the hot ($T > 3$ keV) may be caused by disruptions of magnetic fields associated to a permanent flaring activity.

An FK Comae surface with a 30 to 50 % surface filling factor of bright solar-like active regions could probably explain the X-ray luminosity of its "cool" component. Assuming that this component is produced by a simple static loop system consisting of N similar loops, a characteristic loop length scale L and loop base pressure P can be obtained (see Table 4) from the observed temperature and emission measure of the low count rate period of revolution 205 (see Table 2) using the relation $T = 1400(pL)^{1/3}$ (Rosner, Tucker & Vaiana 1978). Characteristic FK Comae loop size and temperature are respectively 3 10^{10} cm and 8.5 10^6 K. For comparison, solar corona observations show bright hot loops within active regions which reach maximum temperatures and electron densities above the neutral line of typically 3−4 10^6 K and 10^{10} cm^{-3} (Vaiana et al. 1973). In addition to these hot loops, on-disk images of the Sun show that neighboring active regions are often connected into complexes of activity by large loop-like structures (Van Speybroek et al. 1970). These interconnecting loops can be > 10^{10} cm long, i.e. as long as the loop length estimate on FK Comae. However, they tend to be cooler than the loop within solar active region and therefore cooler than coronal loops on FK Comae.

Table 4. Physical parameters of FK Comae coronal loops.

T	EM	L	P	n
K	cm^{-3}	cm	dyn cm^{-2}	cm^{-3}
8.5 10^6	41 10^{52}	3 10^{10}	7	6 10^9

With the straightforward deduction that in FK Comae, the cool plasma component is produced by solar-like active regions covering 30 to 50 % of the star's surface, it is easy to imagine that such a dense population of active regions coexist with constant interaction and disruption of their magnetic fields that might be expected to lead to continuous flaring. This could explain the permanent emission measure contribution of very hot plasma at temperatures of 3 to 5 keV. Assuming that the short transient event during revolution 205 is related to a single flare event, we estimated the parameters of this flare by equating the measured decay time to the radiative cooling time. We then derived a lower limit to the flare emitting volume from the measured emission measure. By further assuming a single loop model with an aspect ratio α=0.1, we roughly estimated the loop length L from the flare emitting volume. We also derived a lower limit to the magnetic field strength by imposing that the flaring structure remains magnetically confined. The resulting values are summarized in Table 5. For comparison purposes, Table 5 also gives observed parameters for solar compact and two ribbon flares (Moore et al. 1980: Wu et al. 1986). For flares cooling predominantly by radiation, there is evidence from our data that the density and the strength of the confining magnetic field is not different from that in solar 2-ribbon flares. The time scale, temperature and density of the X-ray flare on FK Comae are comparable to those observed for 2-ribbon flares on the Sun, while the radiative output and emission measures are three order of magnitude larger. The large release of energy in FK Comae flares would result from a volume effect, i.e from a high number of large magnetic structures interacting in the atmosphere of the star. Direct detections of magnetic fields on a few G-type giants (Hubrig et al. 1994) support the existence of very large scale magnetic structure on stars evolving towards the bottom of the red giant branch.

Table 5. Physical parameters of FK Comae flare during revolution 205 compared with solar flares.

	Solar compact flare	Solar 2-ribbon flare	FK Comae flare
L_X (erg s^{-1})	10^{26}-10^{27}	10^{27}-10^{28}	10^{31}
τ (s)	10^{2}-10^{3}	10^{4}	1.7 10^{4}
T (K)	(1-3) 10^{7}	(1-3) 10^{7}	4 10^{7}
EM (cm^{-3})	10^{48}-10^{49}	10^{49}-10^{50}	$>$ 3.6 10^{52}
n (cm^{-3})	10^{11}-10^{12}	10^{10}-10^{11}	$<$ 5.3 10^{10}
V (cm^{3})	10^{26}-10^{27}	10^{28}-10^{29}	10^{32}
L (cm)	(0.5-5) 10^{9}	10^{10}	2 10^{11}
B_{min} (G)	100-300	50-100	100

7. Conclusion

Our analysis of FK Comae data suggests a scenario where the corona of FK Comae is dominated by the same type of active region structure as on the Sun. However, the surface area coverage of these active regions approaches 50 % and the size of the associated magnetic structure is similar or larger than that of interconnecting loops between solar active regions while their temperature is hotter. The interaction of these structures themselves most likely explains the permanent flaring activity on large scales that is responsible for heating FK Comae plasma to coronal temperatures of $T \geq 10^7$K. These flares are not randomly distributed on the star surface. During our observations, they were partly grouped within a large compact region of about 30 degree extent in longitude. We conjecture that this coronal region with a large density of flares could have been overlaying a giant photospheric spot similar to those mapped using Doppler imaging techniques (Strassmeier et al. 1997).

Acknowledgments. We thank our colleagues from the XMM−Newton Science Operation Center for their support in implementing the observations.

References

Anders, E., & Grevesse, N., 1989, Geochim. Cosmochim. Acta, 53, 197

Bopp B.W., Rucinski S.M., 1981, in IAU Symp. 93, Fundamental Problems in the Theory of Stellar Evolution, ed. D. Sugimoto et al. (Dordrecht: Reidel), p 177.

Favata, F., Schmitt, J. H. M. M., 1999, A&A 350, 900

Golub, L., Pasachoff, J.M., 1997, in The Solar Corona, Cambridge University Press, Cambridge UK.

den Herder, J.W., Brinkman, A.C., Kahn, S.M., et al. 2001, A&A 365, L7

House, L. L., 1969, ApJS, 18, 2

Jansen, F., Lumb, D., Altieri, B., et al. 2001, A&A, 365, L1

Jetsu, L., Pelt, J., Tuominen, I., 1993, A&A 278, 449

Liedahl, D. A., Osterheld, A. L., Goldstein, W. H., 1995, ApJ 438, 115

Makishima, K, 1986, in: The Physics of Accretion onto Compact Objects, p.250, eds. Mason, K. O., Watson, M. G., White, N.,E., Springer Verlag, Berlin.

Mewe, R., Gronenschild, E. H. B., van den Oord, G. H. J., 1985, A&A 62, 197

Mewe, R., Kaastra, J. S.,van den Oord, G. H. J. et al. 1997, A&A 320, 147

Moore, R., McKenzie, D.L., Svesta, Z et al. 1980, in Solar flares, ed. P.A. Sturrock, Colorado Associated University Press, Boulder, CO

Murphy, R.J., Ramaty, R., Reames, D. V. et al. 1991, ApJ 371, 793

Pradhan, A. K, 1982, ApJ 263, 477

Raymond, J. C., Smith, B. W., 1977, ApJS 35, 419

Rosner, R., Tucker, W.H., Vaiana, G.S., 1978, ApJ 220, 643

Schmelz, J. T., 1993, ApJ 408, 373

Strassmaier, K. G., Lupinek, S., Dempsey, R. C. et al. 1999, A&A 347, 212

Strüder, L., Briel, U., Dennerl, K. et al. 2001, A&A, 365, L18

Turner, M. J. L. T., Abbey, A., Arnaud, M., et al. 2001, A&A, 365, L27

Vaiana, G.S., Krieger, A.S., Timothy, A.F., 1973, Sol. Phys. 32, 81

Van Speybroek, L.P., Krieger, A.S., Vaiana, G.S., 1970, Nature 227, 818

Walter, F. M., Basri, G. S., 1982, ApJ 260, 735

Welty, A. D., Ramsey, L. W., 1994, AJ 108, 299